ChemComm

Accepted Manuscript

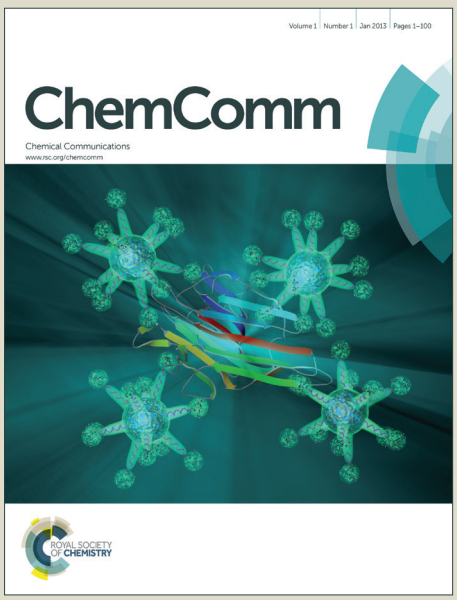

ROYAL SOCIETY OF CHEMISTRY

www.rsc.org/chemcomm

Journal Name

RSCPublishing

COMMUNICATION

On-surface Polymerization on a Semiconducting Oxide: Aryl Halide Coupling Controlled by Surface Hydroxyl Groups on Rutile TiO_2(011)†

Cite this: DOI: 10.1039/xoxxoooooox

Received ooth January 2012,
Accepted ooth January 2012

DOI: 10.1039/xoxxoooooox

www.rsc.org/

Marek Kolmer,*[a] Rafal Zuzak,[a] Amir A. Ahmad Zebari,§[a] Szymon Godlewski,[a] Jakub S. Prauzner-Bechcicki,[a] Witold Piskorz,[b] Filip Zasada,[b] Zbigniew Sojka,[b] David Bléger,[c] Stefan Hecht[c] and Marek Szymonski[a]

Based on scanning tunneling microscopy experiments we show that the covalent coupling of aryl halide monomers on the rutile TiO_2(011)-(2×1) is controlled by the density of surface hydroxyl groups. The efficiency of the polymerization reaction not only depends on the level of surface hydroxylation, but also the presence of hydroxyl groups is essential for the reaction to occur.

On-surface synthesis of covalently bound molecular assemblies in a bottom-up approach has recently become a very attractive field of nanoscience.[1-3] Such strategy allows formation of large variety of well-defined nanostructures including molecular wires,[4-6] 2D molecular networks,[3, 7, 8] or confined graphene nanostructures.[2, 9, 10] On-surface synthesis relies on proper functionalization of the precursor molecules with specific linking sites, which are activated after deposition of the respective monomer building blocks on the surface. To date, surfaces of the coinage metals (Cu, Ag, and Au) were mostly used as substrates, mainly because they essentially facilitate reaction analysis by scanning tunneling microscopy (STM). However, for the sake of practical applications of the on-surface covalent coupling, highly ordered semiconductor[11] or insulator[10, 12] surfaces clearly represent much more attractive platforms. In the case of insulators, covalently bound molecular assemblies are electronically decoupled from the substrate, and hence may serve as independent molecular devices.[5, 13] On the other hand, properly functionalized surfaces of semiconductors, in particular transition metal oxides, offer advantageous optical as well as photo- and electrochemical properties useful in photonics, photocatalysis or gas- and bio- sensing,[14-16] which may benefit from the on-surface polymerized organic semiconductor layer. In this context, titanium dioxide is a profitable inorganic semiconductor, and particularly the surface of rutile TiO_2(011) attracts much attention.[17, 18]

Following our latest report on the feasibility of the on-surface covalent coupling of aryl halide precursors on the rutile TiO_2(011) surface,[11] herein we investigate the role of surface hydroxyl groups and demonstrate univocally that they are essential for the reaction to occur. We show that the polymerization proceeds most effectively when the reduced TiO_2(011) sample is prepared with a moderate density of surface hydroxyls, leading to formation of long molecular oligomers. Increasing the density of the surface hydroxyls by surface exposure to atomic hydrogen results in formation of shorter oligomers, whereas the hydroxyl-free surface suppresses the polymerization reaction completely. The control over the on-surface polymerization by managing the coverage of hydroxyls, exemplified herein by aryl halide coupling on the rutile TiO_2 surface, can most likely be extended to the entire class of transition metal oxides surfaces where acidic hydroxyl groups are present.[19-21] In this regard, our results open an easy, yet powerful route for formation of conjugated organic semiconducting polymers on semiconducting inorganic oxide surfaces.

The (2×1) reconstruction of TiO_2(011) surface (Fig. 1a) consists of two-fold coordinated terminal oxygen and five-fold coordinated terminal titanium atoms forming a characteristic zigzag pattern on the rows running along the [01-1] direction.[22] Hydrogen atom adsorption on the exposed terminal oxygen atoms leads to direct formation of surface hydroxyl groups.[23] In the empty state STM images these surface hydroxyl groups are observed as bright protrusions located non-symmetrically on top of the zigzag pattern (inset in Fig. 1c). To study the role of the surface hydroxyl groups in the on-surface polymerization we prepared a reduced *r*-TiO_2(011)-(2×1) surface containing hydroxyl groups with the less than 0.5% coverage[18] (Fig. 1b), where the coverage is relative to the maximum

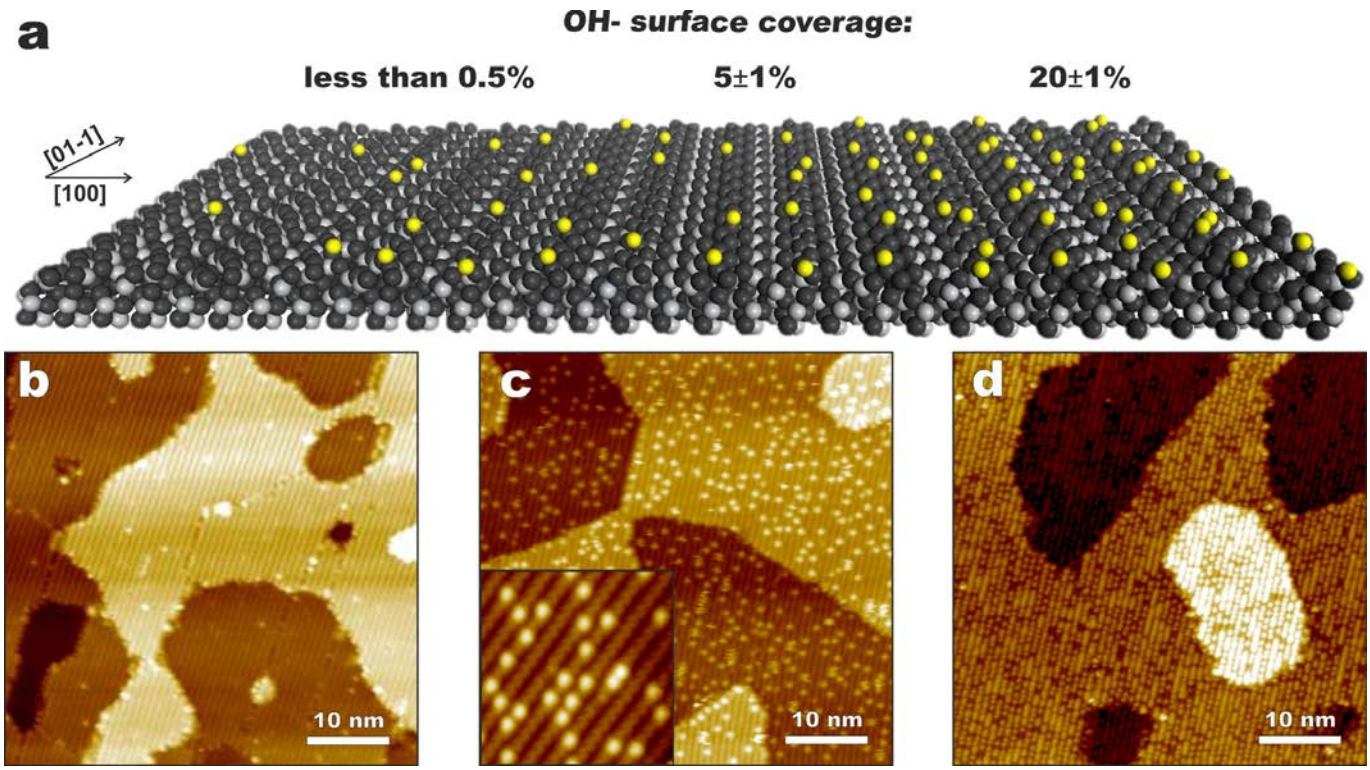

Fig. 1 Rutile surfaces with various hydroxyl group coverage. (a) Model of the TiO_2(011)-(2×1) surface representing substrates with different densities of surface hydroxyls (light gray, dark gray and yellow balls represent Ti, O, and H atoms, respectively). Bottom: STM images of (b) reduced *r*-TiO_2(011), (c) moderately hydroxylated *5%H*-TiO_2(011), and (d) fully hydroxylated *20%H*-TiO_2(011). Inset in (c): high resolution STM image showing surface hydroxyl groups (+1.3 V, 10 pA, 7.5×7.5 nm^2). For all large scale STM images the parameters are +2 V, 10 pA.

number of the available two-fold coordinated terminal oxygen atoms, *i.e.* the full coverage corresponds to 8.0×10^{14} cm^{-2}. The *r*-TiO_2(011) substrate was then used to prepare two other types of well-defined surfaces under ultra-high vacuum conditions. First, we exposed the sample to atomic hydrogen and produced the hydroxylated surfaces. For the purpose of this study, we used a reduced rutile surface with the moderate coverage of 5 ± 1% (*5%H*-TiO_2(011)), shown in Fig. 1c, and with a saturation coverage of 20 ± 1% (*20%H*-TiO_2(011), Fig. 1d). The oxidized *o*-TiO_2(011) surface, in turn, was obtained by annealing the hydroxylated *H*-TiO_2(011) surface in an O_2 atmosphere. This process led to formation of the well-defined surface with low density of the surface hydroxyl groups amounting again to less than 0.5%. As a result, such protocols allow for an effective control over the density of the surface hydroxyl groups and the oxidation state of the substrate as well.

We used the diiodoterfluorene (**DITF**) molecule as a monomer for the on-surface polymerization. Similar monomers bearing two terminal bromine atoms (**DBTF**) have recently been reported to form π-conjugated polymer chains on gold substrates,[4, 6, 24] and investigated with regard to their single molecule charge transport properties. The choice of **DITF** instead of the **DBTF** was motivated by desorption of iodine-related reaction byproducts at elevated temperatures (for details see section 3 in ESI†). Deposition of ~0.3 monolayer (ML) of **DITF** on the *5%H*-TiO_2(011) substrate kept at room temperature gives rise to randomly distributed monomers (Fig. 2a). Comparison of the high resolution experimental STM image (Fig. 2c) with the simulated STM image (Fig. 2d), based on density functional theory (DFT) computational modeling of the **DITF** admolecule structure (Fig. 2b and Fig. S8, ESI†), clearly indicates that the precursor species still preserve their terminal iodine atoms after deposition on the rutile substrate. Indeed, both experimental and simulated STM images exhibit characteristic three central protrusions corresponding to the three dimethyl groups and two smaller lobes at both termini of the admolecules that are attributed to the iodine atoms (*cf.* a terfluorene molecule in Fig S9, ESI†).

To study the influence of the density of the surface hydroxyl groups on the polymerization process, ~0.3 ML of **DITF** monomers was evaporated on the substrates of different hydroxylation extent, all kept at 260 °C (for details see sections 1 and 3 in ESI†). The STM images of the resulting molecular structures (Fig. 3) reveal that on the *r*-TiO_2(011) surface (Fig. 3a and Fig. S5a, ESI†) and the *o*-TiO_2(011) surface (Fig. S5b, ESI†) oligomer formation is quenched. Both substrates have almost no surface hydroxyl groups, and in such a case the **DITF** monomers are found only on the terrace edges and domain boundaries, which are chemically more active than the bare terraces. In particular, the molecules trapped on the domain

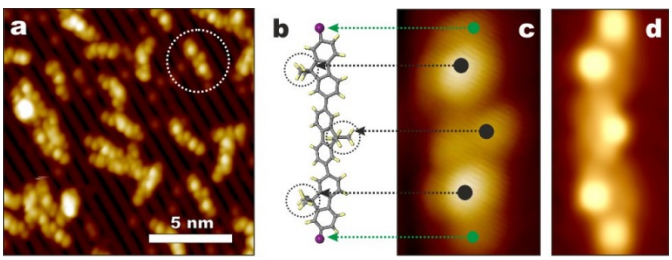

Fig. 2 Depositing the **DITF** monomer on a rutile surface. (a) STM image of **DITF** molecules deposited on *5%H*-TiO_2(011) at room temperature. (b) Model of **DITF** molecule. Iodine atoms are represented by purple balls. (c,d) High resolution experimental (c) and simulated (d) STM images of a single **DITF** molecule on TiO_2(011) (dashed circle in (a)). Black and green dots indicate dimethyl groups and iodine atoms, respectively. For the experimental STM images the parameters are +2 V, 10 pA.

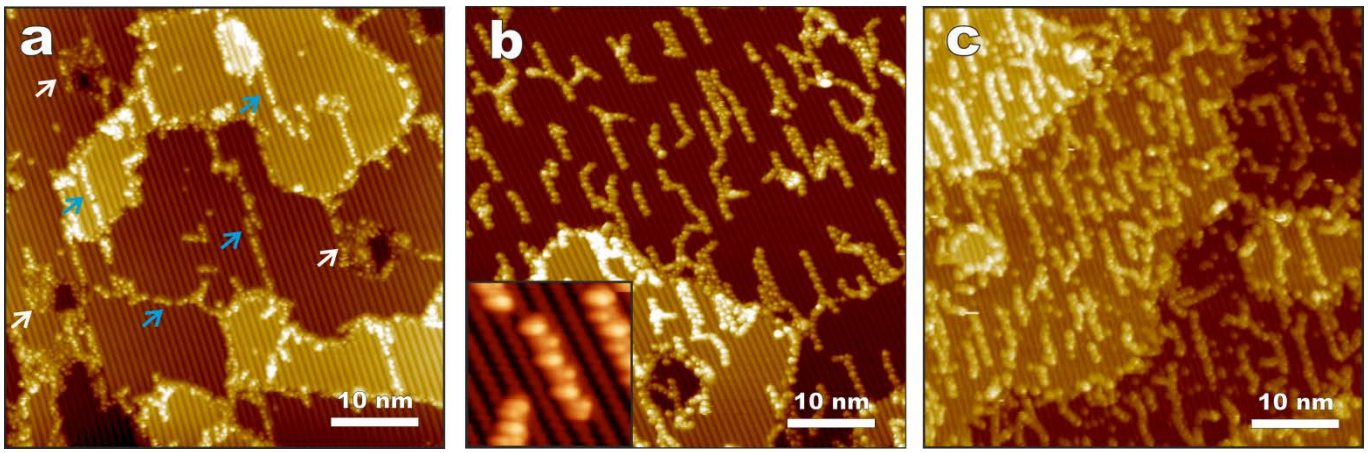

Fig. 3 Polymerizing the **DITF** monomers on rutile surfaces with varying hydroxyl groups coverage. (a) STM image of **DITF** molecules deposited on reduced *r*-TiO_2(011) kept at 260 °C. (b) STM image of **DITF** molecules deposited on moderately hydroxylated *5%H*-TiO_2(011) kept at 260 °C. Inset: high resolution STM image showing a dimer (7×7 nm^2). (c) STM image of **DITF** molecules deposited on fully hydroxylated *20%H*-TiO_2(011) kept at 260 °C. For all STM images the parameters are +2 V, 10 pA. Arrows in (a) point to **DITF** monomers trapped on domain boundaries (blue) and **DITF** forming supramolecular aggregates (white).

boundaries are clearly intact and rather well separated (blue arrows in Fig. 3a), proving that under these conditions the polymerization reaction did not occur. The remaining admolecules form supramolecular aggregates, which are also clearly seen in STM images (white arrows in Fig. 3a). In dramatic variance to these results, evaporation of the **DITF** monomers on the hydroxylated *5%H*-TiO_2(011) and *20%H*-TiO_2(011) substrates leads to formation of well-developed oligomeric species (Fig. 3b and 3c), which are preferentially oriented along the surface reconstruction rows. Analysis of the intramolecular STM contrast of the dimer structure (inset in Fig 3b) proves clearly a covalent coupling between the monomer building blocks. The alternating protrusions along the [01-1] direction, which correspond to the differently oriented dimethyl groups in the polyfluorene chain, all occur with the same separation distance of 0.84 ± 0.01 nm (Fig. S7, ESI†). This value is in agreement with the expected length of a single fluorene unit (0.845 nm).

In the STM images (Fig. 3b and 3c) we also observe a decrease of the density of the surface hydroxyl groups as compared to the substrate state prior to the polymerization. This observation is more evident for the *5%H*-TiO_2(011) surface, where almost no hydroxyl groups remain on the surface, whereas in the case of the *20%H*-TiO_2(011) surface their number is largely reduced, yet they do not vanish completely. It is worth noting here, that simple annealing of the rutile TiO_2(011)-(2×1) at these temperatures does not lead to elimination of the surface-bound hydrogen.[23] Therefore, the spontaneous removal of the surface hydroxyl groups during the course of the polymerization may suggest a potential involvement of the hydrogen atoms in the polymerization process. For example, hydrogen could be involved in the formation of hydrogen iodide as a byproduct of the **DITF** deiodination activating step. Moreover, the oligomers grown on the *5%H*-TiO_2(011) substrate (Fig. 3b) exhibit increased chain lengths as compared to those grown on the *20%H*-TiO_2(011) substrate (Fig. 3c). This qualitative observation is substantiated by statistical analysis of the polymerization reaction products from the detailed inspection of several high resolution STM images (Fig. 4). It proves indeed, that for the *5%H*-TiO_2(011) substrate the oligomers are longer than for *20%H*-TiO_2(011), where the mere dimer structures dominate. Then, the efficiency of the **DIFT** coupling reaction can be described by a conversion parameter, expressed as the ratio (percentage) of the number of monomer connections (C-C bonds) successfully made during the polymerization to the total number of reactive groups (C-I bonds) initially present. The conversion (evaluated using the total number of counted **DITF** monomers N = 901) drops from 55.1 ± 2.5% for *5%H*-TiO_2(011) to 40.1 ± 2.8% for *20%H*-TiO_2(011) (N = 521). The lower efficiency of the reaction leading to the shorter oligomers that take place on the highly hydroxylated substrate, strongly points to the surface hydroxyl groups serving as the key species controlling the polymerization process.

We have recently proposed a tentative multistep proton-assisted mechanism that might be operating during aryl halide coupling leading to polymerization on the hydroxylated TiO_2(011) surface.[11] In this process, proton transfer from the surface hydroxyl group to an adsorbed precursor molecule leads to an activated monomer, which may couple with another, non-activated molecule. After C-C bond formation the proton could remain on the molecule and the process is repeated leading to the oligomerization. All our experimental findings presented here support this proton-induced polymerization

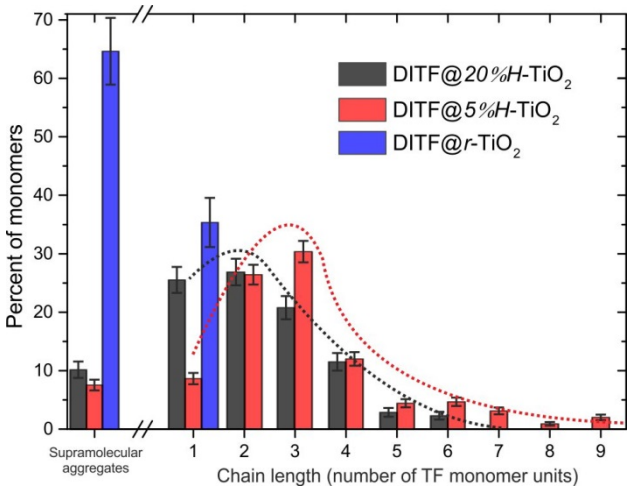

Fig. 4 Oligomer chain length obtained on rutile surfaces with varying hydroxyl groups coverage. Histogram presenting oligomer length on TiO_2(011) surfaces prepared with different densities of hydroxyls after deposition of **DITF** on substrates kept at 260°C. The histogram was obtained from N=198 molecules for *r*-TiO_2(011), N=901 for *5%H*-TiO_2(011) and N=521 for *20%H*-TiO_2(011). The dotted lines are plotted for eye guidance.

mechanism. It nicely explains the observed optimal surface hydroxyl group coverage for the best polymerization outcome, since for coupling to occur the activated, protonated monomers (and growing oligomers) may only react with the intact monomers (due to charge repulsion between the protonated species). Thus the surface hydroxyl coverage, and hence the proton availability, controls the ratio of the activated to non-activated monomers, and thereby the entire polymerization process.

The results of DFT molecular modeling of the on-surface **DITF** coupling confirm the kinetic feasibility of the postulated reaction steps. The energetic barrier for the initial proton transfer is quite low (0.92 eV), and the subsequent coupling proceeds spontaneously with an associated activation energy of 0.98 eV. The activation energies for the analogous coupling of two intact (**DITF-DITF**) and two protonated (**DITF**H^+-**DITF**H^+) molecules are much higher (2.45 eV and 1.95 eV, respectively), accounting well for the experimental observations. The high barrier for the **DITF-DITF** dimerization results from the fact that two inactivated C-I bonds have to be strongly distorted before the formation of C-C bond. In the case of the protonated monomers the acquired charge give rise to their already mentioned strong electrostatic repulsion enhancing the reaction barrier.

In conclusion, we have demonstrated that on a reduced TiO_2(011)-(2×1) surface the efficiency of the coupling reaction between the aryl halides is essentially governed by the density of surface hydroxyl groups. The polymerization process does not occur on the reduced substrate prepared without surface hydroxyls, and is most effective for the TiO_2(011) surface with moderate amount of hydroxyl groups, which is in agreement with a tentative multistep proton-assisted mechanism. Owing to distinctly different nature of transition metal oxides and their much broader structural diversity as compared to metals, our findings open new possibilities for straightforward engineering of hybrid organic-inorganic materials with potentially advantageous properties. These could be controlled by adjusting the valence and conduction bands of the chosen inorganic semiconductor with regard to the HOMO and LUMO levels of the organic semiconductor polymerized directly on top.

This research was supported by the 7th Framework Programme of the European Union Collaborative Project ICT (Information and Communication Technologies) "Atomic Scale and Single Molecule Logic Gate Technologies" (AtMol), contract no. FP7-270028, the Polish Ministry for Science and Higher Education, contract no. 0322/IP3/2013/72, as well as by the German Research Foundation (DFG via SFB 951). The experiment was carried out using equipment purchased with financial support from the European Regional Development Fund within the framework of the Polish Innovation Economy Operational Program (contract no. POIG.02.01.00-12-023/08).

Notes and references

[a] Centre for Nanometer-Scale Science and Advanced Materials, NANOSAM, Faculty of Physics, Astronomy and Applied Computer Science, Jagiellonian University, Lojasiewicza 11, 30-348 Krakow, Poland. E-mail: marek.kolmer@uj.edu.pl.

[b] Faculty of Chemistry, Jagiellonian University, Ingardena 3, 30-060 Krakow, Poland.

[c] Department of Chemistry, Humboldt-Universität zu Berlin, Brook-Taylor-Str. 2, 12489 Berlin, Germany.

† Electronic Supplementary Information (ESI) available. See DOI: 10.1039/c000000x/

§ Present address: Salahaddin University, College of Science, Department of Physics, 44001 Erbil, Kurdistan, Iraq

1. L. Grill, M. Dyer, L. Lafferentz, M. Persson, M. V. Peters and S. Hecht, *Nat. Nanotechnol.*, 2007, **2**, 687-691.
2. J. Cai, P. Ruffieux, R. Jaafar, M. Bieri, T. Braun, S. Blankenburg, M. Muoth, A. P. Seitsonen, M. Saleh, X. Feng, K. Mullen and R. Fasel, *Nature*, 2010, **466**, 470-473.
3. L. Lafferentz, V. Eberhardt, C. Dri, C. Africh, G. Comelli, F. Esch, S. Hecht and L. Grill, *Nat. Chem.*, 2012, **4**, 215-220.
4. L. Lafferentz, F. Ample, H. Yu, S. Hecht, C. Joachim and L. Grill, *Science*, 2009, **323**, 1193-1197.
5. C. Bombis, F. Ample, L. Lafferentz, H. Yu, S. Hecht, C. Joachim and L. Grill, *Angew. Chem. Int. Ed.*, 2009, **48**, 9966-9970.
6. S. Kawai, M. Koch, E. Gnecco, A. Sadeghi, R. Pawlak, T. Glatzel, J. Schwarz, S. Goedecker, S. Hecht, A. Baratoff, L. Grill and E. Meyer, *Proc. Natl. Acad. Sci. U. S. A.*, 2014, **111**, 3968-3972.
7. M. Bieri, M. T. Nguyen, O. Groning, J. M. Cai, M. Treier, K. Ait-Mansour, P. Ruffieux, C. A. Pignedoli, D. Passerone, M. Kastler, K. Mullen and R. Fasel, *J. Am. Chem. Soc.*, 2010, **132**, 16669-16676.
8. J. Eichhorn, D. Nieckarz, O. Ochs, D. Samanta, M. Schmittel, P. J. Szabelski and M. Lackinger, *ACS Nano*, 2014, **8**, 7880-7889.
9. M. Koch, F. Ample, C. Joachim and L. Grill, *Nat. Nanotechnol.*, 2012, **7**, 713-717.
10. C. A. Palma, K. Diller, R. Berger, A. Welle, J. Bjork, J. L. Cabellos, D. J. Mowbray, A. C. Papageorgiou, N. P. Ivleva, S. Matich, E. Margapoti, R. Niessner, B. Menges, J. Reichert, X. L. Feng, H. J. Rader, F. Klappenberger, A. Rubio, K. Mullen and J. V. Barth, *J. Am. Chem. Soc.*, 2014, **136**, 4651-4658.
11. M. Kolmer, A. A. Ahmad Zebari, J. S. Prauzner-Bechcicki, W. Piskorz, F. Zasada, S. Godlewski, B. Such, Z. Sojka and M. Szymonski, *Angew. Chem. Int. Ed.*, 2013, **52**, 10300-10303.
12. M. Kittelmann, P. Rahe, M. Nimmrich, C. M. Hauke, A. Gourdon and A. Kuhnle, *ACS Nano*, 2011, **5**, 8420–8425.
13. J. S. Prauzner-Bechcicki, S. Godlewski and M. Szymonski, *Phys. Status Solidi A*, 2012, **209**, 603-613.
14. U. Diebold, *Surf. Sci. Rep.*, 2003, **48**, 53-229.
15. C. L. Pang, R. Lindsay and G. Thornton, *Chem. Rev.*, 2013, **113**, 3887-3948.
16. M. A. Henderson, *Surf. Sci. Rep.*, 2011, **66**, 185-297.
17. J. Tao, T. Luttrell and M. Batzill, *Nat. Chem.*, 2011, **3**, 296-300.
18. R. Addou, T. P. Senftle, N. O'Connor, M. J. Janik, A. C. T. van Duin and M. Batzill, *ACS Nano*, 2014, **8**, 6321-6333.
19. S. Godlewski, A. Tekiel, J. Budzioch, A. Gourdon, J. S. Prauzner-Bechcicki and M. Szymonski, *ChemPhysChem*, 2009, **10**, 3278-3284.
20. T. P. Trainor, A. M. Chaka, P. J. Eng, M. Newville, G. A. Waychunas, J. G. Catalano and G. E. Brown, *Surf. Sci.*, 2004, **573**, 204-224.
21. F. Traeger, M. Kauer, C. Wöll, D. Rogalla and H. W. Becker, *Phys. Rev. B*, 2011, **84**, 075462.
22. T. Woolcot, G. Teobaldi, C. L. Pang, N. S. Beglitis, A. J. Fisher, W. A. Hofer and G. Thornton, *Phys. Rev. Lett.*, 2012, **109**, 156105.
23. J. Tao, Q. Cuan, X.-Q. Gong and M. Batzill, *J. Phys. Chem. C*, 2012, **116**, 20438-20446.
24. A. Saywell, J. Schwarz, S. Hecht and L. Grill, *Angew. Chem. Int. Ed.*, 2012, **51**, 5096-5100.

